FULL-LENGTH ORIGINAL RESEARCH

Simultaneous subdural and scalp EEG correlates of frontal lobe epileptic sources

***Georgia Ramantani, *Matthias Dümpelmann, †Laurent Koessler, *Armin Brandt, ‡§Delphine Cosandier-Rimélé, ¶Josef Zentner, *Andreas Schulze-Bonhage, and †#**Louis Georges Maillard**

Epilepsia, 55(2):278–288, 2014
doi: 10.1111/epi.12512

Dr. Georgia Ramantani is a child neurologist at the Epilepsy Center, University Hospital Freiburg, Germany.

Summary

Objective: To assess the visibility and detectability in scalp electroencephalography (EEG) of cortical sources in frontal lobe epilepsy (FLE) as to their localization, and the extent and amplitude of activation.

Methods: We analyzed the simultaneous subdural and scalp interictal EEG recordings of 14 patients with refractory frontal lobe epilepsy (FLE) associated with focal cortical dysplasia. Subdural spike types were identified and averaged for source localization and detection of their scalp EEG correlates. Both raw and averaged scalp EEG segments were reviewed for spikes, blinded to subdural segments. We further analyzed the correlation of spike-to-background amplitude ratios in subdural and scalp EEG.

Results: We identified 36 spike types in subdural EEG, corresponding to 29 distinct sources. Four of 29 sources were *visible* by visual evaluation of scalp EEG and six additional sources were *detectable* after averaging: four in the medial frontal, two in the dorsolateral gyri, two in the depth of dorsolateral sulci, and two in the basal frontal region. Cortical sources generating scalp-detectable spikes presented a median of 6 cm^2 of activated cortical convexity surface and a subdural spike-to-background-amplitude ratio >8. These sources were associated with a higher number of activated subdural grid contacts and a higher subdural spike-to-background amplitude ratio than sources generating non–scalp-detectable spikes.

Significance: Not only dorsolateral but also basal and medial sources can be detectable in FLE. This is the first in vivo demonstration derived from simultaneous subdural and scalp EEG recordings of the complementary significance of extensive source activation and higher subdural spike-to-background amplitude ratio in the detection of cortical sources in FLE.

KEY WORDS: Source localization, Intracranial recordings, Refractory epilepsy.

Several in vitro, in vivo, and simulation studies have been conducted to clarify the interrelations of scalp and intracranial electroencephalography (EEG) findings (Abraham & Marsan, 1958; Cooper et al., 1965; Ebersole, 1997; Kobayashi et al., 2005; Tao et al., 2005, 2007; Cosandier-Rimélé et al., 2008). This issue is of cardinal importance in epilepsy management, with scalp EEG constituting a major localizing tool from the primary diagnosis and epilepsy classification to the planning of an intracranial investigation or of a resection in a refractory course. It is noteworthy that previous in vivo studies, both historic and contemporary, have been conducted exclusively in temporal lobe epilepsy (TLE; Abraham & Marsan, 1958; Tao et al., 2005; Ray et al., 2007; Tao et al., 2007). Therefore, there is an imperative need to extend these observations to extratemporal and particularly to frontal lobe epilepsy (FLE), which constitutes a challenge regarding both electroclinical correlations

Accepted November 14, 2013; Early View publication January 13, 2014.
*Epilepsy Center, University Hospital Freiburg, Freiburg, Germany; †Research Center for Automatic Control (CRAN), University of Lorraine, CNRS, UMR 7039, Vandoeuvre, France; ‡INSERM UMR 1099, Rennes, France; §University of Rennes 1, LTSI, Rennes, France; ¶Department of Neurosurgery, University Hospital Freiburg, Freiburg, Germany; #Department of Neurology, Central University Hospital, CHU de Nancy, Nancy, France; and **Medical Faculty, University of Lorraine, Nancy, France

Address correspondence to Georgia Ramantani, Epilepsy Center, University Hospital Freiburg, Breisacher Str. 64, 79106 Freiburg, Germany. E-mail: georgia.ramantani@uniklinik-freiburg.de

(Quesney et al., 1992; Salanova et al., 1993; Bautista et al., 1998) and epilepsy surgery outcomes (Englot et al., 2012).

FLE studies have indeed reported 12–37% of patients without any interictal scalp EEG spikes at all, and a predominance of widespread unilateral or bilateral interictal spikes in the remaining cases (Quesney et al., 1992; Salanova et al., 1993; Bautista et al., 1998; Elsharkawy et al., 2008). Focal interictal spikes have been observed in scalp EEG recordings, mainly in association with dorsolateral frontal sources, whereas medial and orbitofrontal sources have been reported to give rise to bifrontal spikes, if any, with unilateral, albeit often falsely lateralizing, predominance (Quesney et al., 1992; Bautista et al., 1998; Smith et al., 2004). Factors contributing to the disparity between scalp EEG spikes and their cortical substrates include the inaccessibility of large parts of the frontal lobe to scalp electrodes, the extent of intralobar and interlobar connections, and the presence of secondary bilateral synchrony (Kellinghaus & Lüders, 2004).

As a result of this disparity, intracranial recordings still remain mandatory to localize the cortical sources of interictal and ictal discharges in refractory FLE (Englot et al., 2012). In a recent study, we showed that electrical source localization (ESL) derived from subdural interictal EEG spikes in FLE can improve the accuracy of cortical generator localization, both in terms of gyral and deep sulcal resolution (Ramantani et al., 2013b). Simultaneous scalp and intracranial EEG recordings combined with ESL provide a unique opportunity to study the interrelations between cortical generators and their subdural and scalp correlates.

In this study, we aimed to assess the scalp EEG detectability of cortical sources in FLE as delineated by subdural EEG recordings. For this purpose, we retrospectively compared the localization, extent, and amplitude of cortical activation as to the presence of simultaneous scalp EEG correlates. We chose to investigate patients with epilepsy associated with focal cortical dysplasia (FCD; Bast et al., 2006), the prevailing etiology in refractory FLE.

Patients and Methods

Patients

Fourteen patients with refractory FLE associated with FCD and (1) extensive intracranial coverage of the frontal lobe with subdural grid and strip electrodes, (2) simultaneous scalp EEG recordings, (3) technically flawless interictal recording segments of >30 min in calm wakefulness, and (4) clinically validated ESL (Ramantani et al., 2013a), were included in this study. Patients with substantial intracranial hemorrhage or skull defect were excluded. The patient group comprised five male and nine female patients, aged 14–50 years (mean 30). The study was granted approval by the institutional research ethics board. All patients gave their written informed consent.

Methods

EEG recordings and electrode positions

Grid and strip electrode description, placement, and positions were previously reported (Ramantani et al., 2013b). The coverage and number as well as the gyral localization of subdural electrode contacts are given in Table 1.

Simultaneous scalp EEG recordings with electrodes placed according to the 10–20 system (Koessler et al., 2009) using sterile procedures were also available. Occasionally, 1–2 electrodes were slightly displaced from their standard positions to avoid the surgical scars and local edema, usually near the scalp incision in the frontocentral region.

Simultaneous scalp and subdural EEG recordings were obtained using a Neurofile NT digital video-EEG system (Ramantani et al., 2013b).

Interictal spike detection, selection, and analysis

Subdural EEG segments of >30 min in calm wakefulness were carefully chosen to include an adequate number of interictal spikes and avoid ictal events or preictal changes. Sharp transients that appeared less than three times in selected segments, as well as segments of polyspikes (>2 spikes in 200 msec) and activity in the beta or gamma range were visually detected and excluded.

The resulting segments were reviewed using both bipolar and referential montages, and interictal spikes were identified according to the International Federation of Societies for Electroencephalography and Clinical Neurophysiology (1983) recommendations and marked at the time point of their highest amplitude. In view of the multitude of identified interictal spikes, *spike types* were defined to describe spikes of similar spatiotemporal distribution that were presumed to correspond to a single generator. Each spike type was topographically characterized by (1) the dominant contact with maximum amplitude, as defined in a referential montage (Tables 1 and 2), and (2) the amplitude ratio between the spike peak and the mean background activity, calculated in an interval of (−500; −250) and (+250; +500) msec around the peak (Table 2). Subdural EEG spikes of the same type were subsequently averaged to serve for (1) ESL, and (2) detection of their scalp EEG correlates. ESL performed by MUSIC (MUltiple SIgnal Classification; Mosher et al., 1992, 1999) and sLORETA (standardized low-resolution brain electromagnetic tomography; Hämäläinen and Ilmoniemi, 1994; Pascual-Marqui, 2002) was applied to refine the information obtained by visual analysis of subdural spikes and thus served as the reference for localizing their cortical sources, according to the topography of the activation maximum.

Simultaneous scalp and subdural EEG raw segments were separately and independently analyzed by two experienced epileptologists (GR, LGM). In a first step, interictal spikes were annotated in scalp and subdural EEG recordings. Overall, 21–576 spikes (median 194), corresponding to 3–463 (median 91) spikes of each designated spike type, were

Table 1. Frontal lobe subdural electrode coverage and localization of subdural contacts with/without interictal spikes that are detectable/nondetectable in scalp EEG

Patients	Number of subdural contacts	Localization of subdural contacts and spikes											
		Lateral frontal						Medial frontal				Basal frontal	
		Ventral/polar prefrontal	Dorsal prefrontal	Broca/ operculum	Premotor	Primary motor	Medial prefrontal	Anterior cingulate	Premotor	Primary motor	Orbitofrontal		
1	64		■	■	✖	■				■			
2	96	✖	■	✖	■	■	■	■	■	■	✖		
3	94	✖	■	✖	■	✖	■	■	✖	■	✖		
4	84	■	✖		■	■	✖	■	■	■			
5	76		✖		■	■	■	■	◆	■			
6	48		■		◆	■							
7	64		■	■	✖	✖							
8	92	■	✖	■	◆	■	■	■	◆	■			
9	92	■	■			✖	■	■	◆	■			
10	60		✖		■	■	✖	◆	■	■			
11	64		◆		■	■	■	✖	■	■			
12	84	✖	✖		■	■						◆	
13	80	■	◆		■	■	◆			■			
14	90	✖	■	■	■	■	✖	■	■	■		◆	

■: subdural electrode contacts without interictal spikes; ✖: subdural electrode contacts with interictal spikes not visible in scalp EEG; ◆: subdural electrode contacts with interictal spikes visible in scalp EEG.

marked in each subdural EEG segment (Table 2). Spikes presumably arose from a common source when the peaks marked in scalp and subdural EEG recordings were within 10 msec of each other. This interval was chosen because markers were set manually and therefore rather approximately. In a second step, scalp and subdural EEG epochs were averaged using this annotation as a trigger and subsequently analyzed. In all but three cases, at least 10 subdural EEG spikes of each spike type were available for averaging. The first step allowed the identification of scalp spikes with a high spike-to-background amplitude ratio that were *visible* in routine EEG interpretation. The second step allowed the identification of scalp EEG spikes with a low spike-to-background amplitude ratio that were not visible in raw scalp EEG recordings but were rendered *detectable* by averaging.

The *gyral area of cortical activation* corresponding to an interictal EEG spike was estimated as the number of adjacent subdural grid electrode contacts demonstrating concurrent depolarization (Tao et al., 2005). This estimation is relevant solely for convexity sources, sufficiently resolved by the subdural grid contacts. The orbitofrontal and medial frontal regions were sampled by a limited number of irregularly distributed subdural strip contacts, which prohibited an accurate estimation of the spatial extent for interictal spikes originating in these regions. In these latter cases, the gyral area of cortical activation was clearly underestimated, since the sources were located remote from the subdural grid electrodes.

Descriptive and statistical analysis

In a first step, we assessed the source *visibility* in scalp EEG according to their localization as provided by ESL and the visual analysis of subdural recordings (Ramantani et al., 2013b). In a second step, we assessed the source *detectability* in scalp EEG according to the gyral area of cortical activation and spike-to-background amplitude ratio. The number of activated subdural grid contacts and the subdural spike-to-background amplitude ratio was compared between cortical sources generating scalp EEG detectable spikes and cortical sources generating no scalp EEG detectable spikes. We further assessed the correlations between the spike-to-background amplitude ratios of subdural and scalp averaged EEG spikes and the relation of the amplitude of scalp-detectable spikes to the number of activated grid contacts. Finally, we analyzed the spatial distribution of scalp EEG spikes corresponding to detectable cortical sources. Statistical analysis (Wilcoxon signed-rank test) was conducted using R version 2.15.1 (R Foundation for Statistical Computing, Vienna, Austria). The significance level for all tests was set at $p < 0.05$.

Results

Localization of intracerebral sources

Visual analysis of subdural recordings revealed 36 spike types in 14 patients, with an average of three spike types per

Table 2. Characteristics of cortical sources in all 14 patients with frontal lobe epilepsy, including their anatomic localization, the localization of dominant contacts, the number of subdural contacts involved in the electrical field, the amplitude and spike-to-background amplitude ratio of subdural EEG spikes, the visibility of their scalp EEG correlates, the number of averaged subdural EEG spikes of each spike type, and the resulting detectability of their scalp EEG correlates as well as the amplitude and spike-to-background amplitude ratio of corresponding scalp EEG spikes. The numbers in column 1 refer to the corresponding patients, as presented in Table 1

Sources	Sublobar localization of dominant subdural contacts	Number of subdural contacts		Subdural EEG spike amplitude (μV)	Subdural EEG spike to background amplitude ratio	Raw scalp EEG visibility	Number of averaged subdural EEG spikes	AVG scalp EEG detectability	Simultaneous scalp EEG spike amplitude, μV	Scalp EEG spike to background amplitude ratio
		Dorsolateral	Medial/basal							
Medial frontal sources										
3/R premotor medial SFG	Medial premotor		2	93	8.2	No events	143	No events		
5/L premotor medial SFG	Medial premotor	3	6	197	9.8	No events	97	C4/Fz/Cz	8	0.4
8/L premotor medial SFG	Medial premotor	4		226	20.3	No events	18	No events		
9/L premotor medial SFG	Medial premotor	6	2	145	51.0	No events	463	C3/**Cz**/Pz/P3	5	1.9
5/L prefrontal medial SFG	Lateral dorsal prefrontal	8		252	14.0	No events	97	No events		
10/L motor cingulate gyrus	Medial prefrontal/anterior cingulate	5	4	150	15.6	No events	141	Cz	4	0.5
11/L anterior cingulate gyrus	Anterior cingulate		3	257	17.1	No events	117	No events		
	Anterior cingulate		4	165	4.4	No events	44	No events		
	Lateral dorsal prefrontal	14	6	380	13.0	No events	32	Fp2/F4/C4/ Fz/Cz/Pz	50	1.2
Basal/orbitofrontal sources										
2/R basal lateral/OF	Lateral ventral prefrontal/basal OF	2		154	8.3	No events	111	No events		
3/R basal lateral/OF	Basal OF		2	207	24.2	No events	177	No events		
	Lateral ventral prefrontal	2		269	19.1	No events	158	No events		
12/L lateral basal/polar/OF	Basal OF		3	274	21.5	No events	22	No events		
12/L medial basal/polar/OF	Basal OF		4	141	9.7	FP1/F7	70	FP1/F7/T3	6	0.4
14/L medial basal OF	Basal OF		3	143	7.8	No events	157	FP1/**F7**/T3	11	0.7
Dorsolateral sulcal sources										
9/L motor depth of central sulcus	Lateral primary motor	4		276	19.7	No events	10	No events		
7/R motor depth of central sulcus	Lateral primary motor	5		160	16.8	No events	55	No events		
1/R premotor depth of SFS	Lateral premotor	7		178	11.4	No events	21	No events		
7/R premotor depth of SFS	Lateral premotor	6		223	5.1	No events	5	No events		
8/L premotor depth of SFS	Lateral premotor	2		43	3.0	No events	18	No events		
	Lateral premotor	11		341	28.9	Cz/Pz/C3/P3	40	**Pz**/**Cz**/C3/P3/F3	19	2.0
	Medial premotor	5		203	18.9	No events	16	**Cz**/C3/Pz	12	1.4
4/R prefrontal depth of SFS	Lateral dorsal/medial prefrontal	4	2	187	4.7	No events	331	No events		
8/L prefrontal depth of SFS	Lateral dorsal prefrontal	7		268	12.1	No events	32	No events		
14/L prefrontal depth of SFS	Lateral ventral prefrontal	2		254	16.5	No events	138	No events		
	Medial prefrontal		2	115	3.9	No events	28	No events		

Continued

Epilepsia, 55(2):278–288, 2014
doi: 10.1111/epi.12512

Table 2. Continued.

Sources	Sublobar localization of dominant subdural contacts	Number of subdural contacts		Subdural EEG spike amplitude (μV)	Subdural EEG spike to background amplitude ratio	Raw scalp EEG visibility	Number of averaged subdural EEG spikes	AVG scalp EEG detectability	Simultaneous scalp EEG spike amplitude, μV	Scalp EEG spike to background amplitude ratio
		Dorsolateral	Medial/basal							
13/R prefrontal dorsal lateral SFS	Medial prefrontal	8	4	116	39.4	No events	161	Fz	4	1.4
	Lateral dorsal prefrontal	5	3	616	27.2	Fz	395	Fz/**Cz**	5	0.3
7/R prefrontal depth of IFS	Lateral premotor	6		108	7.1	No events	18	No events		
Dorsolateral gyral sources										
2/R central operculum	Operculum	4		193	4.2	No events	30	No events		
3/R central operculum	Primary motor operculum	2		255	8.2	No events	15	No events		
2/R premotor operculum	Operculum	6		198	19.0	No events	183	No events		
6/R premotor lateral in MFG	Lateral premotor	8		162	20.0	No events	172	C4/C3/**Cz**/Pz/P3/P4	6	1.0
10/L prefrontal MFG	Lateral dorsal prefrontal	2		203	5.6	No events	8	No events		
12/L lateral/ventral/polar MFG	Lateral dorsal/ventral prefrontal	2		248	16.4	No events	4	No events		
13/R prefrontal dorsal lateral SFG	Lateral dorsal prefrontal	8	5	538	65.7	Fz/Cz	20	Fz	14	1.5

AVG, average; SFG, superior frontal gyrus; SFS, superior frontal sulcus; OF, orbito-frontal region; IFS, inferior frontal sulcus; MFG, middle frontal gyrus.

patient (range 1–5), corresponding to 29 distinct cortical sources (Table 2). All sources were localized within subdural electrode coverage. Seven sources were localized in the medial frontal gyri (Fig. 1), seven in dorsolateral gyri, 10 in the depth of dorsolateral sulci (Fig. 2), and five in the basal or orbitofrontal gyri (Fig. 3).

Twenty-eight of 29 sources were adjacent to the dominant subdural contact. However, 5 of these 28 sources also corresponded to an additional spike type with a dominant subdural contact remote to the source. Three of these five sources were localized in the depth of the superior frontal sulcus and generated spikes visible on both lateral and medial subdural contacts, one was localized in the orbitofrontal region and generated spikes visible on both basal and lateral ventral contacts, and one was located in the anterior cingulate gyrus and generated spikes visible on both medial and lateral contacts. The only source fully remote from the dominant contact was localized in the medial aspect of the superior frontal gyrus, whereas the dominant contact was lateral prefrontal (Table 2).

Source visibility and detectability in scalp EEG in relation to their localization

Only 4 of 29 cortical sources produced spikes *visible* by routine visual evaluation of simultaneous raw scalp EEG recordings (Table 2): two sources localized in the superior frontal sulcus, one in the superior frontal gyrus, and one in the orbitofrontal region (Figs. 2 and 3).

After averaging, 10 of 29 (six additional) sources were *detectable*: 4 of 7 in the medial frontal, 2 of 7 in the dorsolateral gyri, 2 of 10 in the depth of dorsolateral sulci, and 2 of 5 in the basal-frontal regions (Table 2). Two of four detectable medial frontal sources were localized in the premotor medial aspect of the superior frontal gyrus, and two in the cingulate gyrus (Fig. 1); none were visible before averaging. One of two detectable dorsolateral gyral sources was localized in the superior frontal gyrus and was visible before averaging, and one was localized in the middle frontal gyrus and was not visible before averaging. Both detectable dorsolateral sulcal sources were localized in the depth of the superior frontal sulcus (Fig. 2) and were visible before averaging. Both detectable frontobasal sources were localized in the medial polar orbitofrontal cortex, and one was visible before averaging (Fig. 3).

Source detectability in scalp EEG in relation to the extent and amplitude of dorsolateral cortical activation

Subdural EEG spikes detectable in simultaneous scalp EEG presented a 116–616 μV amplitude and an 8–66 spike-to-background amplitude ratio. The number of subdural grid contacts involved in scalp-detectable cortical spikes were 0–14 (median 6), thus roughly corresponding to a cortical convexity activation of 0–14 cm^2. In contrast, subdural EEG spikes not detectable in scalp EEG presented a

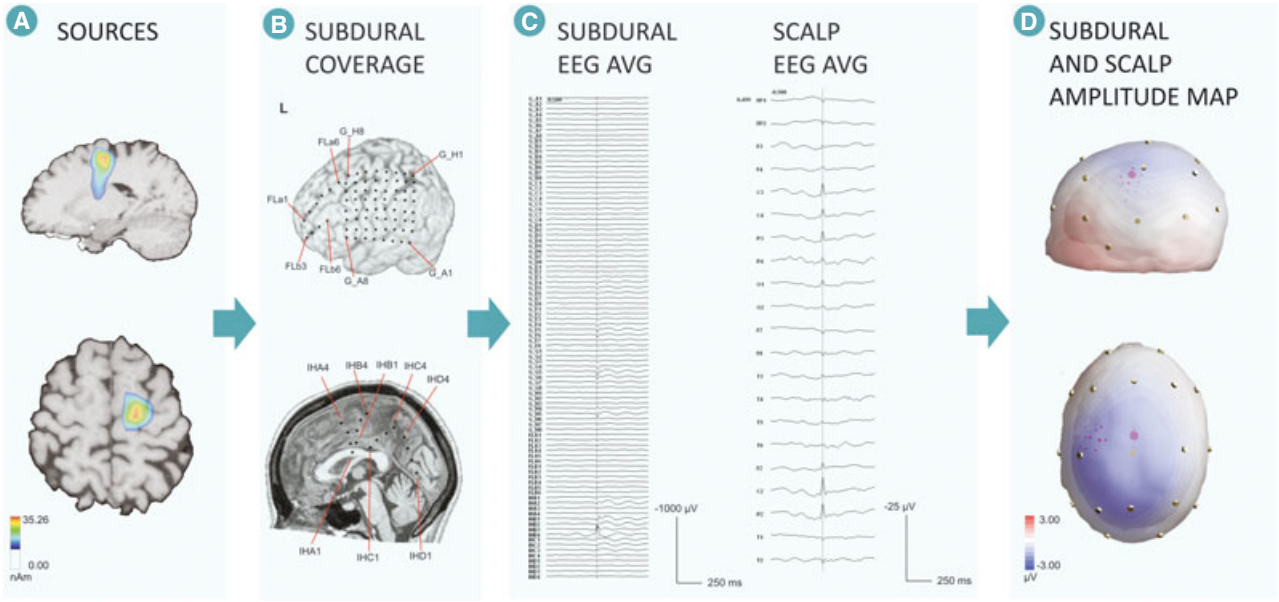

Figure 1.
Patient 9, with a premotor source localized in the medial part of the left superior frontal gyrus. Illustration of the source reconstruction by MUSIC (**A**), the subdural electrode coverage (**B**), subdural EEG and scalp EEG averaged spikes (**C**), and the 3D overlay of the subdural and scalp amplitude map (**D**), with the sphere diameters corresponding to the amplitude of the subdural EEG spike. The subdural EEG average, presenting an activation of six dorsolateral and two medial contacts, corresponds to a bilateral frontocentral averaged scalp EEG spike, with the highest amplitude in electrodes Cz/Pz/C3/P3.

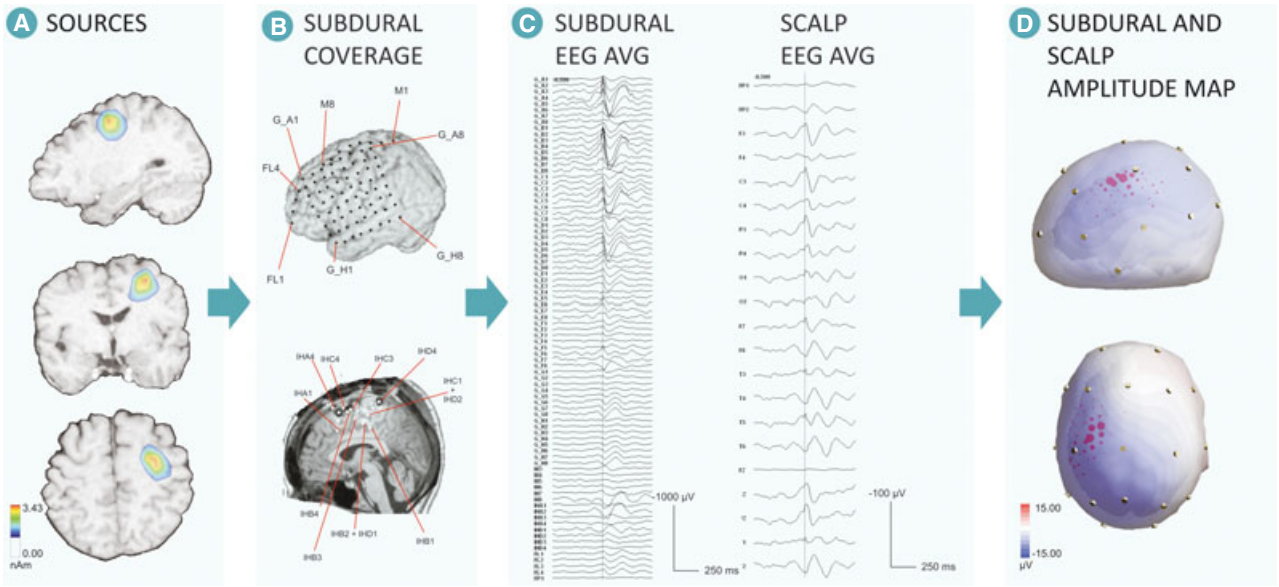

Figure 2.
Patient 8, with a dorsolateral premotor source localized in the depth of the left superior frontal sulcus. Illustration of the source reconstruction by MUSIC (**A**), the subdural electrode coverage (**B**), subdural EEG and scalp EEG averaged spikes (**C**), and the 3D overlay of the subdural and scalp amplitude map (**D**), with the sphere diameters corresponding to the amplitude of the subdural EEG spike. The subdural EEG average, presenting an activation of 11 dorsolateral subdural contacts, corresponds to a left and medial frontocentral and parietal averaged scalp EEG spike, with the highest amplitude in electrodes Cz/Pz/F3/C3/P3.

43–276 µV amplitude range and a 3–24 spike-to-background amplitude ratio and involved 0–8 subdural grid contacts (median 2).

The number of activated subdural grid contacts and the subdural spike-to-background amplitude ratio were significantly higher ($p < 0.001$ and $p = 0.002$, respectively) for

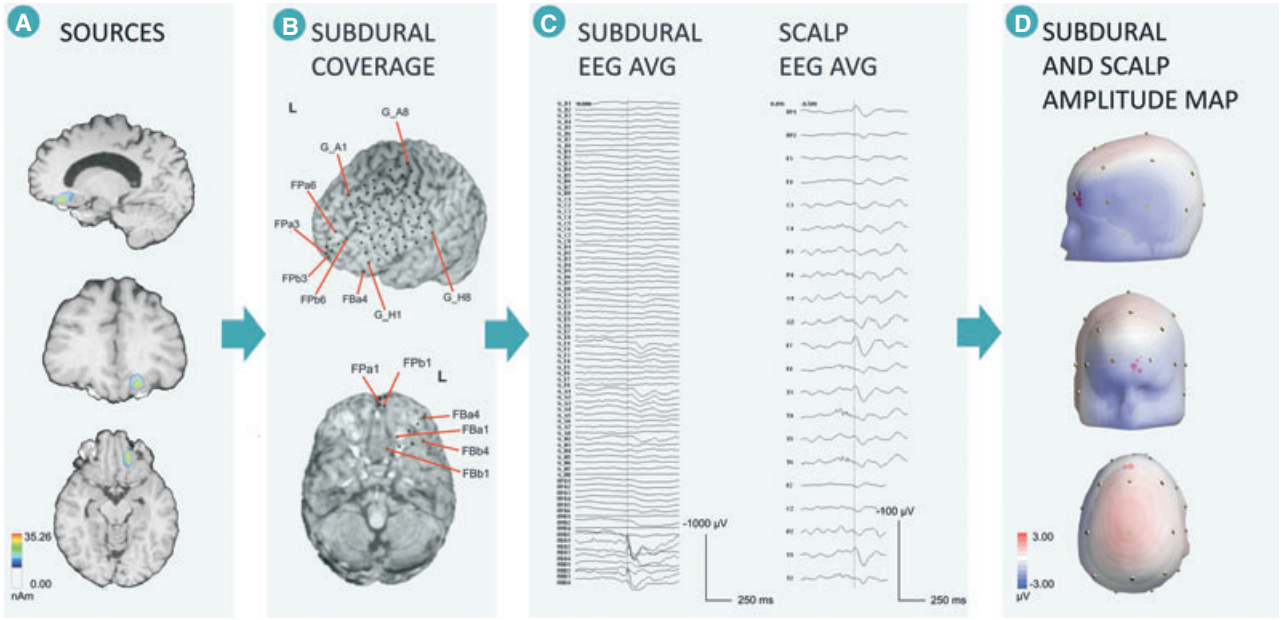

Figure 3.
Patient 12, with a mesial orbitofrontal source localized in the medial and polar part of the left orbitofrontal cortex. Illustration of the source reconstruction by MUSIC (**A**), the subdural electrode coverage (**B**), subdural EEG and scalp EEG averaged spikes (**C**), and the 3D overlay of the subdural and scalp amplitude map (**D**), with the sphere diameters corresponding to the amplitude of the subdural EEG spike. The subdural EEG average, presenting an activation of four frontobasal subdural contacts, corresponds to a bilateral left predominant frontopolar, basal and temporal scalp EEG average spike, with the highest amplitude in electrodes Fp1, F7, T3.

sources generating scalp-detectable spikes compared to sources generating no scalp-detectable spikes. The respective subdural and scalp spike-to-background amplitude ratios of scalp-detectable spikes were strongly correlated (Fig. S1; $p = 0.002$). Furthermore, the amplitude of averaged scalp-detectable spikes was related to the number of activated grid contacts ($p < 0.001$).

Spatial distribution of detectable cortical sources in scalp EEG

All four detectable medial frontal sources (two in the cingulate gyrus and two in the medial part of the superior frontal gyrus) projected to midline dominant scalp electrodes (Cz in four cases with additional Fz and Pz in two cases). Additional ipsilateral or contralateral frontocentral scalp electrodes were involved in one and two cases, respectively. Both orbitofrontal sources generating scalp-detectable spikes (Fig. 3) projected to ipsilateral frontopolar and temporal electrodes (Fp1, F7, T3). Moreover, detectable dorsolateral sources localized in the superior frontal gyrus or in the superior frontal sulcus projected to midline electrodes (Fz, Cz, or Pz) in all three cases and involved additional ipsilateral frontal-centroparietal electrodes (F3, C3, P3) in one case (Fig. 2). The remaining detectable gyral dorsolateral source localized in the middle frontal gyrus and projected to additional bilateral centroparietal scalp electrodes. In this last case, a careful analysis of the temporal dynamics of the scalp spike showed a 20 msec delay between the spikes recorded on C3 and C4, thus suggesting that the right scalp spike was related to propagation rather than to volume conduction from the left middle frontal gyrus source to the contralateral scalp electrodes.

Discussion

The identification of the cortical sources of EEG constitutes a fundamental issue in electrophysiology, and the matching of scalp signals to their cortical substrates is an important key in decoding these complex source-signal interrelations (Abraham & Marsan, 1958; Tao et al., 2005, 2007). To our knowledge, our study is the first to analyze simultaneous subdural and scalp EEG recordings in FLE to address the issue of cortical substrates for scalp spikes. Furthermore, this represents the first attempt to use both visual analysis and ESL of subdural EEG recordings in refining the localization and adding a three-dimensional (3D) perception of cortical substrates.

Visibility of sources in raw scalp EEG

In our study, we showed that most frontal lobe sources failed to generate scalp-visible spikes. Indeed, only 14% sources had scalp EEG correlates *visible* in routine analysis. This is much lower than the 63–88% rates previously reported in nonsimultaneous subdural- and scalp-EEG recordings (Quesney et al., 1992; Salanova et al., 1993; Bautista et al., 1998; Elsharkawy et al., 2008). This cannot

be attributed to the limited spatial 10–20 scalp-sampling that was also applicable to all previous studies. This discrepancy may be due to a selection bias related to the improved magnetic resonance imaging (MRI) detection of epileptogenic lesions such as FCD nowadays. These patients may present more spatially limited irritative zones, less likely to generate interictal EEG scalp spikes *visible* in routine interpretation. Moreover, this discrepancy is largely related to methodologic issues, since past studies compared the results of nonsimultaneous scalp- and subdural-EEG recordings, thus preventing accurate spatial correlations between the cortical substrates of scalp and subdural spikes, while increasing the probability of sampling interictal spikes. On the other hand, in simultaneous scalp- and subdural-EEG recordings, the attenuation effect of the silastic membrane of the grid may account for lower spike visibility (Lanfer et al., 2013). However, this effect has been minimized in our study by carefully inspecting and selecting scalp EEG segments for the absence of amplitude asymmetry.

In line with previous reports (Quesney et al., 1992; Salanova et al., 1993; Bautista et al., 1998), three of four scalp-visible interictal EEG spikes in our study corresponded to sources localized in the *lateral* convexity, particularly in the superior frontal sulcus or superior frontal gyrus. Only one case of a scalp-visible interictal EEG spike corresponded to a *medial* orbitofrontal and polar source.

Overall detectability of sources in averaged scalp EEG

After averaging of subdural interictal EEG spikes, six additional sources were rendered *detectable* in scalp-EEG. Averaging allows increasing the signal-to-noise ratio by attenuating the background activity and thus the contribution of nonepileptic cortical sources (Abraham & Marsan, 1958). This suggests that the very low visibility of FLE interictal sources is partly linked to cortical activity generated in adjacent regions (Ramantani et al., 2006). The significance of this was emphasized recently in a study using a realistic model of cortical and scalp EEG generation at seizure onset (Cosandier-Rimélé et al., 2012). Our study is the first to quantitatively assess this parameter in vivo, in the context of FLE. The elimination of background activity revealed not only medial or basal frontal but also dorsolateral cortical sources that would otherwise be undetectable in scalp EEG. However, it should be noted that averaging did not enhance detectability when applied to <10 subdural EEG spikes, as was the case in three spike types corresponding to dorsolateral cortical sources.

It is important to note that in our study, there were no systematically detectable or undetectable cortical source localizations. Indeed, even spikes originating from sources adjacent to the convexity may be missed by scalp recordings. Conversely, 8 of 22 sources in the medial frontal gyri, in the depth of dorsolateral sulci, or in the orbitofrontal cortex were detectable, whereas these regions have been reported to generate spikes escaping routine scalp EEG interpretation (Quesney et al., 1992; Salanova et al., 1993; Bautista et al., 1998; Smith et al., 2004). The detectability of mesial frontal as well as orbitofrontal sources may be partly attributed to the breach effect of the overlying craniotomy in simultaneous scalp- and subdural-EEG recordings. However, this still constitutes an important finding, especially since we have largely counteracted this effect by ruling out patients with substantial skull defects.

Detectability and scalp EEG correlates of medial frontal sources

Two of four medial detectable sources were located in the medial premotor aspect of the superior frontal gyrus, and two in the cingulate gyrus. Sources restricted to medial frontal lobe structures are believed to be less detectable due to the horizontal orientation of resulting neuronal currents and the distance to the frontocentral scalp electrodes (Bautista et al., 1998). In our study, however, these sources did not present a lower detectability compared to lateral convexity sources. Three medial detectable sources were located in the premotor areas, including the mid-cingulate motor cortex. The specific cytoarchitectonic characteristics of this agranular cortex—and especially of the mid-cingulate cortex, with a high density of pyramidal cells in layer V (Vogt et al., 2003), as well as its highly functional cortico-cortical connections facilitating the rapid spread of epileptic discharges, may account for this detectability (Matsumoto et al., 2007). All detectable medial sources had a common projection on midline electrodes, reflecting the fact that their spatial geometry was not purely vertical, but corresponded to a more complex 3D configuration involving the banks of medial sulci, such as the cingulate sulcus. These sources involved additional frontocentral scalp electrodes in three cases: these were either ipsilateral, or contralateral and falsely lateralized, in line with previous reports (Quesney et al., 1992; Salanova et al., 1993; Bautista et al., 1998; Smith et al., 2004; Elsharkawy et al., 2008).

Detectability and scalp EEG correlates of orbitofrontal sources

Another two detectable sources were orbitofrontal, of altogether five sources localized in this region. Sources restricted to medial orbitofrontal structures have been presumed undetectable in scalp EEG recordings, due to the vertical orientation of the neuronal currents and the resulting equivalent dipole, the distance to the overlying frontal scalp electrodes, and the absence of recording contacts below the orbitofrontal plane (Gavaret et al., 2006). However, this latter study derived from nonsimultaneous scalp and intracerebral EEG recordings. In our study, subdural EEG spikes corresponding to both detectable orbitofrontal sources were restricted to basal strip electrodes, lacking concomitant grid activation, and thus rendering propagation to the lateral convexity improbable. This observation strongly suggests that sources restricted to the medial

orbitofrontal cortex can be detectable in scalp EEG, in line with a previously reported case of orbitofrontal spikes recorded by depth-electrode contacts occurring simultaneously with scalp-visible spikes (Merlet & Gotman, 1999). Of interest, both detectable orbitofrontal sources had a common projection to ipsilateral frontotemporal electrodes (Fp1, F7, T3), as reported for two of four patients with orbitofrontal epilepsy in a previous study (Smith et al., 2004). The previously described bifrontal pattern in relation to orbitofrontal sources (Ludwig et al., 1975; Merlet & Gotman, 1999; Smith et al., 2004) was not observed in our study.

Detectability and scalp EEG correlates of dorsolateral sulcal or gyral sources

Overall, 4 of 17 dorsolateral sources generated scalp-detectable spikes, including 2 of 7 gyral and 2 of 10 sulcal sources. The comparable detectability of gyral and sulcal dorsolateral sources in our study is in contrast to the perception that gyral sources with their predominantly radial voltage fields present optimal scalp EEG detectability, whereas sulcal sources with their predominantly tangential voltage fields are less detectable in scalp EEG. This lack of predominance of gyral sources in terms of scalp EEG detectability may be partly attributed to their more pronounced attenuation by the silastic membrane of the grid, compared to deeper sources (Lanfer et al., 2013). Therefore, considering the gyral dorsolateral sources, the only source localized in the superior frontal gyrus and one of three sources in the middle frontal gyrus, but none of the opercular sources, were detectable. Considering sulcal dorsolateral sources, both sources located in the superior frontal sulcus, but none in the inferior frontal and central sulcus, were detectable. Moreover, detectable sources localized in the superior frontal gyrus or in the superior frontal sulcus projected to dominant midline electrodes (Fz, Cz, Pz) in all three cases and involved additional lateralized frontal-centroparietal scalp electrodes in one case. The remaining detectable gyral dorsolateral sources were localized in the middle frontal gyrus and projected to additional bilateral centroparietal scalp electrodes. Altogether, sources lateral to the superior frontal gyrus projected to both midline and lateral scalp electrodes that were ipsilateral rather than falsely lateralizing, in contrast to medial sources. Finally, contrary to the common perception of predominantly widespread interictal spikes in FLE (Kellinghaus & Lüders, 2004), these were limited to three or fewer scalp electrodes in the majority of detectable sources. This may be attributed to the enhanced detectability of spatially limited sources after averaging. Indeed, these sources may have been overlooked in previous studies that relied on only routine visual interpretation.

Source visibility and detectability according to the extent and amplitude of dorsolateral cortical activation

In our study, the majority of interictal spikes recorded from subdural electrodes were not *detectable* in the simultaneous scalp EEG after averaging, regardless of source localization. This underscores the contribution of parameters other than source localization, including the extent and amplitude of cortical activation, to the interrelations between intracerebral sources and their scalp correlates. We specifically addressed the contribution of the extent and amplitude of cortical activation to the scalp EEG correlates of sources projecting to dorsolateral grid electrode contacts. No assessment of this particular contribution for the generation of scalp-EEG spikes has been undertaken in the context of FLE to date. The extent of cortical activation can be roughly estimated from the number of activated contacts, and the amplitude of cortical activation can be estimated from the subdural spike-to-background amplitude ratio, provided that a neocortical source is adjacent to and covered by the subdural grid electrodes (Abraham & Marsan, 1958; Tao et al., 2005). In the present study, we showed that both the number of activated subdural grid contacts and the spike-to-background amplitude ratio were significantly higher for sources generating scalp-detectable spikes. The median cortical activation extent of 6 cm^2 corresponding to scalp-detectable sources in our study is comparable to the seminal in vitro estimation in the absence of background activity (Cooper et al., 1965) that has been widely cited and partly corroborated by simulation studies (Kobayashi et al., 2005). It is, however, lower than the 10–20 cm^2 cortical activation extent derived from more recent in vivo and in vitro studies in TLE (Tao et al., 2005; Cosandier-Rimele et al., 2008). The discrepancy of our estimates to the latter values may be partly attributed to the variable lobar localization considered in each of the two in vivo studies (Cooper et al., 1965; Tao et al., 2005). However, it most probably underscores the difference between sources that are *visible* in routine visual interpretation and sources that are *detectable* only after averaging, resulting from the interaction between the cortical activation extent and the blurring effect of the surrounding cortical activity (Tao et al., 2005). In our study, averaging indeed attenuated the blurring effect of the background activity and thus probably enhanced the detectability of spatially limited cortical sources. We further showed that the subdural spike-to-background amplitude ratios were significantly higher for sources generating scalp-detectable spikes and established a strong correlation between the spike-to-background amplitude ratios of subdural and scalp spikes, thus demonstrating the significance of cortical spike amplitude on source detectability.

Limitations of the study

With the disparity between scalp and subdural EEG recordings partly accounted for by the impedance of the dura, skull, and scalp, there are two further technical issues constituting inherent limitations in establishing accurate correlations. Although the bone flap was carefully replaced following the implantation of the subdural grid electrodes, the craniotomy could produce a breach effect resulting in

higher amplitudes of scalp EEG potentials through the abolition of spatial filtering by skull bone. On the other hand, the silastic membrane of the subdural grid constitutes an additional layer over the cortical areas of interest that could result in further attenuation of scalp signals (Lanfer et al., 2013). Because both conditions would result in either enhancement or local attenuation of both epileptic interictal spikes and background activity in scalp EEG, segments were carefully inspected and selected for the absence of amplitude asymmetry. Furthermore, as mentioned in the Methods section, patients with significant skull defects or those with subdural or epidural hemorrhage interfering with the quality of the recordings were excluded. Nonetheless, despite inherent limitations, simultaneous scalp and subdural recordings offer a unique chance to study the correlations of scalp EEG spikes with their cortical substrates in epilepsy patients, taking advantage of the superior spatial resolution of subdural grids.

Conclusion

Our study showed that not only dorsolateral but also orbitofrontal and medial-frontal sources can be detectable in scalp EEG. This work constitutes the first in vivo demonstration based on simultaneous subdural and scalp EEG recordings and the first quantitative assessment of the complementary significance of extensive source activation and higher subdural spike-to-background amplitude ratio in the detection of epileptic generators in FLE. This contributes to the decoding of interrelations between cortical sources and their scalp EEG correlates. The appreciation of these interrelations is indeed of cardinal importance for the development and validation of new diagnostic tools such as electrical source localization derived from scalp EEG, magnetoencephalography (MEG), or EEG–functional MRI (fMRI) that may constitute a surrogate for invasive recordings in the future (Bast et al., 2005; Koessler et al., 2010; Jacobs et al., 2013). This is particularly relevant for FCD that represents the main substrate of surgically remediable neocortical partial epilepsy (Bast et al., 2006). Indeed, surgical outcomes in FCD-associated epilepsy, contrary to other cortical malformations (Ramantani et al., 2013a), are strongly related to the complete removal of the epileptogenic lesion that can be reliably localized by the analysis of its interictal activity.

Acknowledgments

The authors would like to express their gratitude to the medical technicians of the Epilepsy Center Freiburg (Carolin Gierschner, Andre Haak, Christiane Lehmann, Anika Schinkel, Verena Schulte, and Mandy Wenzel) for their valuable assistance.

Disclosure

None of the authors has any conflict of interest to disclose. We confirm that we have read the Journal's position on issues involved in ethical publication and affirm that this report is consistent with those guidelines.

References

Abraham K, Marsan CA. (1958) Patterns of cortical discharges and their relation to routine scalp electroencephalography. *Electroencephalogr Clin Neurophysiol* 10:447–461.

Bast T, Ramantani G, Boppel T, Metzke T, Ozkan O, Stippich C, Seitz A, Rupp A, Rating D, Scherg M. (2005) Source analysis of interictal spikes in polymicrogyria: loss of relevant cortical fissures requires simultaneous EEG to avoid MEG misinterpretation. *Neuroimage* 25:1232–1241.

Bast T, Ramantani G, Seitz A, Rating D. (2006) Focal cortical dysplasia: prevalence, clinical presentation and epilepsy in children and adults. *Acta Neurol Scand* 113:72–81.

Bautista RE, Spencer DD, Spencer SS. (1998) EEG findings in frontal lobe epilepsies. *Neurology* 50:1765–1771.

Cooper R, Winter AL, Crow HJ, Walter WG. (1965) Comparison of subcortical, cortical and scalp activity using chronically indwelling electrodes in man. *Electroencephalogr Clin Neurophysiol* 18:217–228.

Cosandier-Rimélé D, Merlet I, Badier JM, Chauvel P, Wendling F. (2008) The neuronal sources of EEG: modeling of simultaneous scalp and intracerebral recordings in epilepsy. *Neuroimage* 42:135–146.

Cosandier-Rimélé D, Bartolomei F, Merlet I, Chauvel P, Wendling F. (2012) Recording of fast activity at the onset of partial seizures: depth EEG vs. scalp EEG. *Neuroimage* 59:3474–3487.

Ebersole JS. (1997) Defining epileptogenic foci: past, present, future. *J Clin Neurophysiol* 14:470–483.

Elsharkawy AE, Alabbasi AH, Pannek H, Schulz R, Hoppe M, Pahs G, Nayel M, Issa A, Ebner A. (2008) Outcome of frontal lobe epilepsy surgery in adults. *Epilepsy Res* 81:97–106.

Englot DJ, Wang DD, Rolston JD, Shih TT, Chang EF. (2012) Rates and predictors of long-term seizure freedom after frontal lobe epilepsy surgery: a systematic review and meta-analysis. *J Neurosurg* 116:1042–1048.

Gavaret M, Badier JM, Marquis P, McGonigal A, Bartolomei F, Regis J, Chauvel P. (2006) Electric source imaging in frontal lobe epilepsy. *J Clin Neurophysiol* 23:358–370.

Hämäläinen MS, Ilmoniemi RJ. (1994) Interpreting magnetic fields of the brain: minimum norm estimates. *Med Biol Eng Comput* 32:35–42.

Jacobs J, Stich J, Zahneisen B, Assländer J, Ramantani G, Schulze-Bonhage A, Korinthenberg R, Hennig J, Levan P. (2013) Fast fMRI provides high statistical power in the analysis of epileptic networks. *Neuroimage* Oct 18 [Epub ahead of print].

International Federation of Societies for Electroencephalography and Clinical Neurophysiology. (1983) *Recommendations for the Practice of Clinical Neurophysiology*. Elsevier, Amsterdam.

Kellinghaus C, Lüders HO. (2004) Frontal lobe epilepsy. *Epileptic Disord* 6:223–239.

Kobayashi K, Yoshinaga H, Ohtsuka Y, Gotman J. (2005) Dipole modeling of epileptic spikes can be accurate or misleading. *Epilepsia* 46:397–408.

Koessler L, Maillard L, Benhadid A, Vignal JP, Felblinger J, Vespignani H, Braun M. (2009) Automated cortical projection of EEG sensors: anatomical correlation via the international 10-10 system. *Neuroimage* 46:64–72.

Koessler L, Benar C, Maillard L, Badier JM, Vignal JP, Bartolomei F, Chauvel P, Gavaret M. (2010) Source localization of ictal epileptic activity investigated by high resolution EEG and validated by SEEG. *Neuroimage* 51:642–653.

Lanfer B, Röer C, Scherg M, Rampp S, Kellinghaus C, Wolters C. (2013) Influence of a silastic ECoG grid on EEG/ECoG based source analysis. *Brain Topogr* 26:212–228.

Ludwig B, Marsan CA, Van Buren J. (1975) Cerebral seizures of probable orbitofrontal origin. *Epilepsia* 16:141–158.

Matsumoto R, Nair DR, LaPresto E, Bingaman W, Shibasaki H, Lüders HO. (2007) Functional connectivity in human cortical motor system: a cortico-cortical evoked potential study. *Brain* 130:181–197.

Merlet I, Gotman J. (1999) Reliability of dipole models of epileptic spikes. *Clin Neurophysiol* 110:1013–1028.

Mosher JC, Lewis PS, Leahy RM. (1992) Multiple dipole modeling and localization from spatio-temporal MEG data. *IEEE Trans Biomed Eng* 39:541–557.

Mosher JC, Baillet S, Leahy RM. (1999) EEG source localization and imaging using multiple signal classification approaches. *J Clin Neurophysiol* 16:225–238.

Pascual-Marqui RD. (2002) Standardized low-resolution brain electromagnetic tomography (sLORETA): technical details. *Methods Find Exp Clin Pharmacol* 24(Suppl. D):5–12.

Quesney LF, Constain M, Rasmussen T, Stefan H, Olivier A. (1992) How large are frontal lobe epileptogenic zones? EEG, ECoG, and SEEG evidence. *Adv Neurol* 57:311–323.

Ramantani G, Boor R, Paetau R, Ille N, Feneberg R, Rupp A, Boppel T, Scherg M, Rating D, Bast T. (2006) MEG versus EEG: influence of background activity on interictal spike detection. *J Clin Neurophysiol* 23:498–508.

Ramantani G, Koessler L, Colnat-Coulbois S, Vignal JP, Isnard J, Catenoix H, Jonas J, Zentner J, Schulze-Bonhage A, Maillard LG. (2013a) Intracranial evaluation of the epileptogenic zone in regional infrasylvian polymicrogyria. *Epilepsia* 54:296–304.

Ramantani G, Cosandier-Rimélé D, Schulze-Bonhage A, Maillard L, Zentner J, Dümpelmann M. (2013b) Source reconstruction based on subdural EEG recordings adds to the presurgical evaluation in refractory frontal lobe epilepsy. *Clin Neurophysiol* 124:481–491.

Ray A, Tao JX, Hawes-Ebersole SM, Ebersole JS. (2007) Localizing value of scalp EEG spikes: a simultaneous scalp and intracranial study. *Clin Neurophysiol* 118:69–79.

Salanova V, Morris HH III, Van Ness PC, Lüders H, Dinner D, Wyllie E. (1993) Comparison of scalp electroencephalogram with subdural electrocorticogram recordings and functional mapping in frontal lobe epilepsy. *Arch Neurol* 50:294–299.

Smith JR, Sillay K, Winkler P, King DW, Loring DW. (2004) Orbitofrontal epilepsy: electroclinical analysis of surgical cases and literature review. *Stereotact Funct Neurosurg* 82:20–25.

Tao JX, Ray A, Hawes-Ebersole S, Ebersole JS. (2005) Intracranial EEG substrates of scalp EEG interictal spikes. *Epilepsia* 46:669–676.

Tao JX, Baldwin M, Ray A, Hawes-Ebersole S, Ebersole JS. (2007) The impact of cerebral source area and synchrony on recording scalp electroencephalography ictal patterns. *Epilepsia* 48:2167–2176.

Vogt BA, Berger GR, Derbyshire SW. (2003) Structural and functional dichotomy of human midcingulate cortex. *Eur J Neurosci* 18:3134–3144.

Supporting Information

Additional Supporting Information may be found in the online version of this article:

Figure S1. Correlation between subdural and scalp spike-to-background-amplitude ratios of scalp-detectable sources (Wilcoxon test: $p = 0.002$).